Promoting Effect of Chloride on the SO_2 Adsorption Capacity and Adsorption Rate of Alumina-Supported Copper Oxide Adsorbents: Thermogravimetric and Infrared Studies

Svetlana Iretskaya

Apyron Technologies, Inc., Atlanta, Georgia 30340

Mark B. Mitchell*

Department of Chemistry and the Center for Surface Chemistry, Clark Atlanta University, Atlanta, Georgia 30314

Received: November 6, 2002; In Final Form: January 2, 2003

Alumina-supported copper oxide materials were examined for their capacity to adsorb SO_2 from a SO_2/O_2/He gas stream at relatively low temperature (150 °C). The adsorbent (8 wt % copper oxide) was treated with a series of different compounds to examine the promoting effect of chloride and other halides and alkali metals. The results show that chloride has a strong promoting influence on both the rate of adsorption and the total capacity for SO_2 on copper oxide on alumina adsorbents. When chloride is used to promote adsorbents formed using copper oxide as a precursor, the mode of promotion is apparently one wherein the chloride acts to facilitate the wetting of the alumina surface by the copper oxide and/or copper sulfate species. The result is the formation of extended networks of copper oxide that are stable for many adsorption/regeneration cycles. Adsorbents formed in this fashion are more reactive for sulfur dioxide adsorption than adsorbents containing similar amounts of well-dispersed copper oxide formed using copper nitrate as a precursor.

Introduction

Sulfur oxide (SO_x) emissions from combustion processes present a critical emissions control problem, both in terms of the contributions of sulfur oxides to acid rain as well as the effects of sulfur oxides on emissions control systems for NO_x. The current study is focused on the significant increase in the adsorption capacity and reaction rate of SO_2 on alumina-supported copper oxide materials at relatively low temperatures (150 °C) that occurs with added chloride. While many of the applications of SO_2 abatement technology involve gas streams at temperatures in excess of 300 °C, there is a significant need for SO_2 control technology at lower temperatures. For diesel engine applications, there are significant portions of the warm-up period during which the emission gas temperature is much less than 300 °C, even as low as 75 °C. Also, the temperature requirements associated with SO_2 abatement technology applied to power plant emissions place significant restrictions on the type of system used, the placement of the ductwork, etc. Expanding the temperature range over which SO_2 abatement technology is effective will broaden its application and make its use more cost-effective.

Copper oxide on aluminum oxide solid-state materials have been studied for many years for their ability to adsorb and react with SO_x, sequestering sulfur oxides very effectively.[1−6] Evidence suggests that a surface copper oxide species catalyzes the oxidation of SO_2 to SO_3 by gas-phase oxygen. The SO_3 then reacts with copper oxide to form a copper sulfate. At temperatures in excess of 250 °C, the SO_3 is relatively mobile on the surface and can migrate to a neighboring aluminum oxide to form a surface aluminum sulfate species:[1,2,4,5]

$$SO_2 + 1/2\ O_2 + CuO_{(surf)} \leftrightarrow CuO\text{-}SO_{3(surf)} \quad (1)$$

$$CuO\text{-}SO_{3(surf)} \rightarrow CuSO_{4(surf)} \quad (2)$$

$$CuO\text{-}SO_{3(surf)} + AlO_{(surf)} \rightarrow CuO + AlSO_{4(surf)} \quad (3)$$

$CuO_{(surf)}$ is an active surface copper species, $CuO-SO_{3(surf)}$ is a chemisorbed SO_3, $AlO_{(surf)}$ is a surface aluminum species, and $CuSO_{4(surf)}$ and $AlSO_{4(surf)}$ are surface sulfate species associated with copper and aluminum, respectively. The participation of the support can lead to a much higher adsorption capacity for SO_2 than can be realized by the formation of copper sulfate alone. The degree of participation of the support in the sequestration of sulfur dioxide increases with increasing reaction temperature. At 500 °C, the majority of the sulfur dioxide adsorption capacity is associated with the formation of bulk aluminum sulfate.[2,4]

The adsorption capacity due to the copper species can be virtually completely regenerated by treatment with a reducing gas, e.g., CH_4 or H_2, at modest temperatures, 400−500 °C, followed by oxidation of the surface copper by gas-phase oxygen to regenerate the active surface species

$$CuSO_{4(surf)} + 1/2\ CH_4 \rightarrow Cu_{(surf)} + SO_2 + 1/2\ CO_2 + H_2O \quad (4)$$

$$Cu_{(surf)} + 1/2\ O_2 \rightarrow CuO_{(surf)} \quad (5)$$

Regeneration of bulk aluminum sulfate is more difficult, and its formation can lead to a loss of capacity as a function of adsorption/regeneration cycle.[1,4]

* To whom correspondence should be addressed. E-mail: mmitchel@cau.edu. Phone: 404-880-6860. Fax: 404-880-6890.

10.1021/jp0274029 CCC: $25.00
Published on Web 05/06/2003

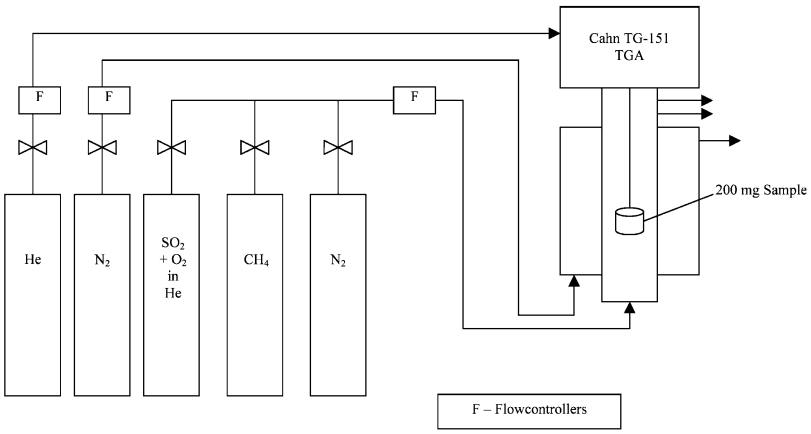

Figure 1. Schematic diagram of the Cahn TG-151 TGA system used for adsorption/regeneration measurements. Helium is used to purge the weighing mechanism to protect it from the reactive gases. A nitrogen flow is used to purge the space between the heating coils and the quartz reactor tube. The reaction gases flow in from the bottom of the system, through the adsorbent, and out to the exhaust or analysis system along with the helium from the TGA purge.

TABLE 1: Alumina-Supported Copper Oxide Adsorbents Examined

name	copper source	acid used	Cu:promoter mole ratio	promoter for posttreatment	multi-point BET surface area, (m^2/g)
CuO − N. P.	CuO	7% HOAc	N/A	none	229.8
CuO−HCl	CuO	2% HCl	2:1	none	230.5
CuO−HNO_3	CuO	6.3% HNO_3	N/A	none	228.9
$Cu(NO_3)_2$ − N. P.	$Cu(NO_3)_2$	none	N/A	none	225.6
$Cu(NO_3)_2$ − HCl	$Cu(NO_3)_2$	HCl	2:1	none	226.5
CuO − LiCl	CuO	7% HOAc	2:1	LiCl	253.6
CuO − NaCl	CuO	7% HOAc	2:1	NaCl	240.3
CuO − KCl	CuO	7% HOAc	2:1	KCl	232.2
CuO − KBr	CuO	7% HOAc	2:1	KBr	237.1
CuO − KF	CuO	7% HOAc	2:1	KF	231.2
CuO − KI	CuO	7% HOAc	2:1	KI	250.3
CuO − KNO_3	CuO	7% HOAc	2:1	KNO_3	235.7
CuO − NH_4Cl-2	CuO	7% HOAc	2:1	NH_4Cl	241.9
CuO − NH_4Cl-5	CuO	7% HOAc	5:1	NH_4Cl	247.3
CuO − NH_4Cl-20	CuO	7% HOAc	20:1	NH_4Cl	244.9

Experimental Section

Sample Preparation. The samples were synthesized using a patented co-particle technology developed by Apyron Technologies, Inc., and were provided by Apyron Technologies.[7,8] CuO (BET surface area 0.1 m^2/g), alumina (261 m^2/g), and colloidal aluminum hydroxide (322 m^2/g) were mixed together with dilute acid, and the mixture was subsequently dried and calcined at 500 °C. All samples discussed in this manuscript contained approximately 8 wt % CuO after calcining.

Two other adsorbents were prepared using $Cu(NO_3)_2$ as the copper source. The alumina and colloidal aluminum hydroxide were mixed together as powders, and the $Cu(NO_3)_2$ was added as an aqueous solution using incipient wetness impregnation. One of the $Cu(NO_3)_2$ adsorbents contained no further additives, whereas the other was promoted with HCl by replacing some of the water needed in the impregnation step with dilute HCl. The samples were prepared to contain the same amount of copper as the materials prepared using CuO (8 wt % CuO) and were dried and calcined in the same fashion. Elemental analysis of some of the samples for sulfur content was carried out by Galbraith Laboratories, Knoxville, TN. Routine elemental analysis of the samples for copper content was carried out in-house using a Perkin-Elmer Elan 5000 ICP-MS.

The $CuSO_4/Al_2O_3$ reference materials for infrared analysis were prepared by dissolving $CuSO_4$ in water (to yield an amount of copper equivalent to 1 wt % CuO or 8 wt % CuO) and then impregnating the alumina with this solution by incipient wetness. The samples contained approximately 2 wt % $CuSO_4$ or 15 wt % $CuSO_4$. The reference samples were dried overnight at 70 °C, but were not calcined.

Addition of Promoters to CuO/Al_2O_3 Adsorbents. For the examination of the effects of the different promoters, the adsorbent prepared with acetic acid was used as the starting material. This material was impregnated with the promoters using incipient wetness. Aqueous solutions designed to yield specific final Cu:promoter mole ratios were used for the impregnations. The samples examined are listed in Table 1.

Thermogravimetric Analysis. Pure gases for the adsorption/regeneration experiments were purchased from Holox and were ultrahigh purity grade. The sulfur dioxide certified gas mixture was purchased from Matheson Gas.

The sulfur dioxide adsorption capacities and adsorption rates of the different materials were measured using a Cahn TG-151 thermogravimetric analyzer (TGA). A diagram of the instrumental setup is shown in Figure 1. A sample weighing approximately 200 mg was placed in the weighing basket (wire mesh, 250 μm aperture, 60 μm diameter wire) of the TGA that allowed flow of the reactive gases through the adsorbent. The thermocouple sits just below the sample basket. The temperature and weight are recorded in real time by computer through a serial interface with the TGA electronics.

For typical measurements of sulfur dioxide adsorption, the sample was first purged in nitrogen and then reduced by heating in pure methane to 500 °C. After 15 min at this temperature,

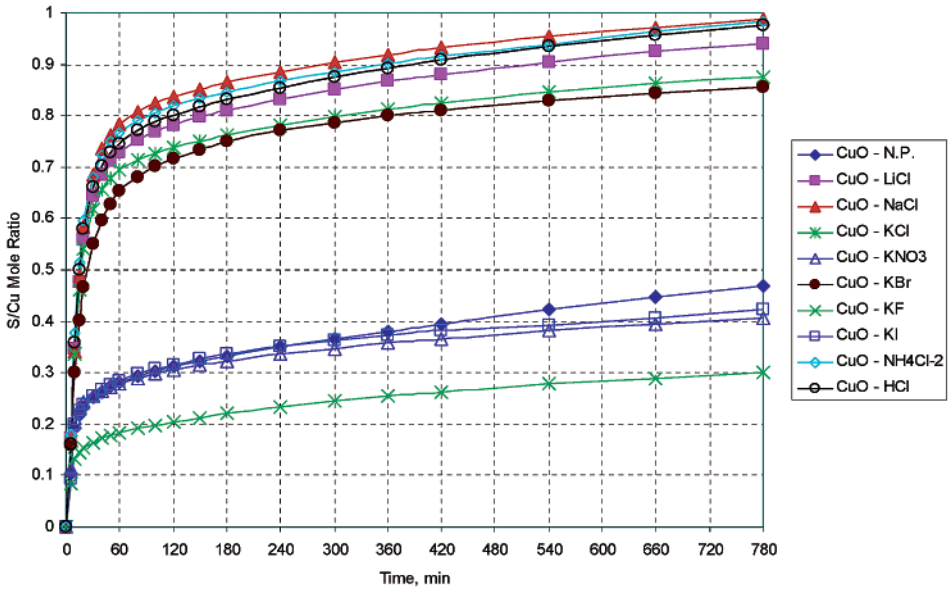

Figure 2. Adsorption of SO_2 (for the third adsorption cycle) by a series of copper oxide on alumina (8 wt % copper oxide) adsorbents posttreated with different promoters. The reaction conditions are $T = 150$°C, $[SO_2] = 0.3\%$ (vol), $[O_2] = 2\%$ (vol).

the reactant gas flow was switched to nitrogen, and the sample was cooled to 150 °C. The reactant gas flow was switched to the SO_2 adsorption mixture (3000 ppm SO_2, 2 vol % O_2, balance He), and the adsorption was carried out for a specified time, typically 30 min, occasionally overnight for 13−16 h. After this exposure, the reactant gas was switched to nitrogen to purge the sample and then switched to methane and the sample heated to 500 °C to accomplish the regeneration. After 15 min, the reactant gas was switched to nitrogen, the sample cooled to 150 °C, and the process repeated.

Infrared Analysis. The infrared diffuse reflectance spectroscopy measurements of the adsorbents were carried out using a Nicolet Magna 750 FT-IR, with a Harrick Scientific DRA-2 diffuse reflectance optical accessory and HVC-DR2 environmental cell. The ex situ infrared spectra of the adsorbents sulfated by exposure to the SO_2/O_2 mixture for 13 h in the TGA apparatus were obtained by placing the sample in the sample cup of the DRIFTS cell and acquiring a spectrum. No special sample treatment was used. The background spectrum used was a spectrum of KBr. A sample of the adsorbent before exposure to the SO_2/O_2 mixture was used to generate a reference spectrum that was subtracted from the spectrum of the sulfated adsorbent.

The in situ infrared spectroscopy of the adsorbent exposed to probe molecules, CO and NO, is carried out as follows. The adsorbent powder was placed in the controlled environment chamber and heated to approximately 300 °C in a slowly flowing mixture of 20% O_2 in helium for 30 min to evolve any water, CO_2, or organics that may have adsorbed after preparation of the sample. The sample was then cooled to room temperature, and a background spectrum was measured. For the CO adsorption experiments, CO (research grade) from Holox was used, and the samples were exposed to 200 Torr CO for 10 min, after which time the spectrum was measured. For the NO experiments, 1% NO in He (to minimize the formation of NO_2 and N_2O during storage) purchased from Matheson was used as the adsorption gas, and the sample was exposed to 300 Torr of this mixture. For each of the probe molecules, a spectrum of the pure support material in the presence of the probe molecule was measured and subtracted from the spectrum of the probe molecule interacting with the copper oxide adsorbents.

Results

Thermogravimetric Analysis (TGA) Experiments. Early in our investigation of these materials for SO_2 adsorption capacity, it became clear that the materials formed with HCl performed significantly better in the presence of O_2 than those formed with either HNO_3 or CH_3COOH, although the improved performance was not observed in the absence of oxygen. The strength of the acids alone could not account for the differences. One possibility to be investigated was that the chloride ion was somehow promoting the activity of the adsorbent in the presence of oxygen.

A scheme was developed to examine the effects of a variety of different possible promoters on the capacity of the adsorbent. The method involved starting with an adsorbent formed using dilute acetic acid, modifying the adsorbent by posttreating with different possible promoters, and examining the effects of the promoters on the adsorption/regeneration properties of the adsorbents. A series of halogens and other alkali metal salts were evaluated to determine their effect on the SO_2 adsorption capacity. Figure 2 shows the results of those determinations. The results clearly show that chloride addition to the alumina-supported copper oxide adsorbent yields adsorbents with the highest adsorption capacity. Of the other halides tested, only bromide showed a significant positive effect on SO_2 adsorption. The adsorption stoichiometry used in Figure 2 assumes that the form of copper after the reduction step is Cu^0 and that the final form after adsorption and reaction is $CuSO_4$, with all of the additional oxygen coming from the gas phase. It appears that the chloride promoted copper oxide adsorbents approach a limiting adsorption stoichiometry (S:Cu) of approximately 1:1. The S:Cu ratios have been confirmed by elemental analysis of several samples after completing TGA experiments.

These results clearly indicate that the chloride itself is responsible for the enhanced adsorption properties of the adsorbent, rather than the acid or the alkali. Further evidence for this interpretation is given by experiments that examined the SO_2 adsorption as a function of chloride concentration (Figure 3). For the experiments represented in Figure 3, the chloride was added by posttreating adsorbents prepared using

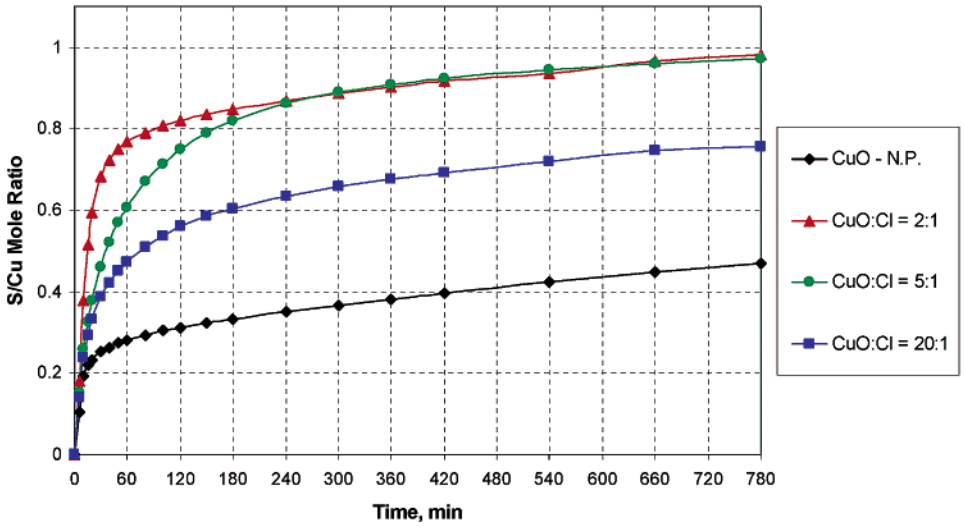

Figure 3. Adsorption of SO_2 (for the third adsorption cycle) by four different CuO adsorbents as a function of Cu:Cl mole ratio. The adsorbents examined were CuO−N.P., CuO−NH_4Cl-2, CuO−NH_4Cl-5, and CuO−NH_4Cl-20. The reaction conditions are as in Figure 2.

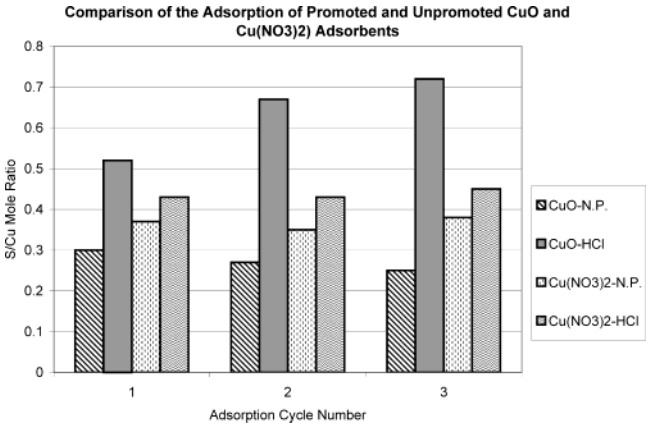

Figure 4. Comparison of the SO_2 uptake for four different adsorbents: the unpromoted and HCl-promoted CuO adsorbents, and the unpromoted and HCl-promoted $Cu(NO_3)_2$ adsorbents (8 wt % CuO, 150 °C, 30 min. adsorption time).

acetic acid with solutions of NH_4Cl to obtain the appropriate Cu:Cl ratio. As can be seen, even an adsorbent with a Cu:Cl mole ratio of 20:1 shows a significant improvement in adsorption capacity compared to one not treated with chloride.

As a way of examining the involvement of enhanced dispersion in the chloride promotion effect, two additional solids were examined. One was a copper oxide/alumina adsorbent prepared using $Cu(NO_3)_2$ without further promotion, and the other was a similar material promoted with HCl to yield a Cu:Cl ratio of 2:1. These materials are referred to as the $Cu(NO_3)_2$ adsorbents. A comparison of the uptake of SO_2 by these two materials with that of chloride-promoted and unpromoted copper oxide adsorbents formed using CuO as the copper source (referred to as the CuO adsorbents) is shown in Figure 4. The amount of SO_2 adsorbed increases as a function of adsorption cycle for the promoted CuO adsorbent, whereas the amount adsorbed decreases for the unpromoted adsorbent. The adsorption capacities observed for both of the CuO adsorbents are found to stabilize after the third cycle, whereas the $Cu(NO_3)_2$ adsorbents show no evolution in the adsorption capacity as a function of adsorption cycle, although the chloride-promoted $Cu(NO_3)_2$ adsorbent shows enhanced SO_2 uptake relative to the unpromoted $Cu(NO_3)_2$ adsorbent.

A series of experiments was carried out to examine the effects of chloride and sodium independently on the SO_2 adsorption

TABLE 2: Effect of Additives on the SO_2 Adsorption Capacity of Alumina (Percent Weight Gain)

additive	1st adsorption cycle	2nd adsorption cycle	3rd adsorption ycle
none	2.0	1.48	1.54
HCl	1.35	1.14	1.39
NaCl	1.96	1.68	1.88
$NaNO_3$	2.8	1.46	1.48

capacity of alumina containing no copper. The alumina samples examined were prepared and treated exactly as for the copper oxide on alumina experiments. For all of these experiments, the additive being examined was added to the alumina using incipient wetness, with a loading of 0.5 mmol/g, a loading equivalent to the chloride loading used for the majority of the chloride-impregnated experiments with the CuO/Al_2O_3 adsorbents (2:1 Cu:Cl). Adsorbents comprised of alumina alone and alumina impregnated with either HCl, NaCl, or $NaNO_3$ were examined and compared for their SO_2 adsorption capacity in exactly the same fashion as the copper-containing adsorbents. The SO_2 adsorption observed for 30 min exposure, expressed as wt % increase relative to the weight at the beginning of each adsorption cycle, is shown for three successive adsorption cycles in Table 2. For comparison, the weight gain for the unpromoted CuO/Al_2O_3 adsorbent for the first cycle was found to be 2.4 wt % (Figure 4). As can be seen from Table 2, none of the additives has a positive impact on the SO_2 uptake of alumina except for $NaNO_3$. As our group and others have observed in the past, added sodium increases the SO_2 adsorption capacity of alumina.[9,10,11] However, the results observed here indicate that the increase in SO_2 uptake at 150 °C for the sodium-impregnated alumina is only observed for the first cycle. The decrease in adsorption capacity for the sodium-impregnated alumina for cycles after the first is thought to be due to the loss of adsorption sites to the formation of sodium sulfate on the surface, which is more difficult to regenerate.[9]

Chloride also has a positive effect on the SO_2 adsorption capacity of copper oxide on other support materials, though not as dramatic as that found for copper oxide on alumina. On a ZrO_2/Al_2O_3 support, the amount of adsorbed SO_2 increases approximately 70% for a similar supported copper oxide adsorbent promoted with chloride (8 wt % Cu as CuO, Cu:Cl ratio of 2.5:1), whereas on a silica support, the enhancement is

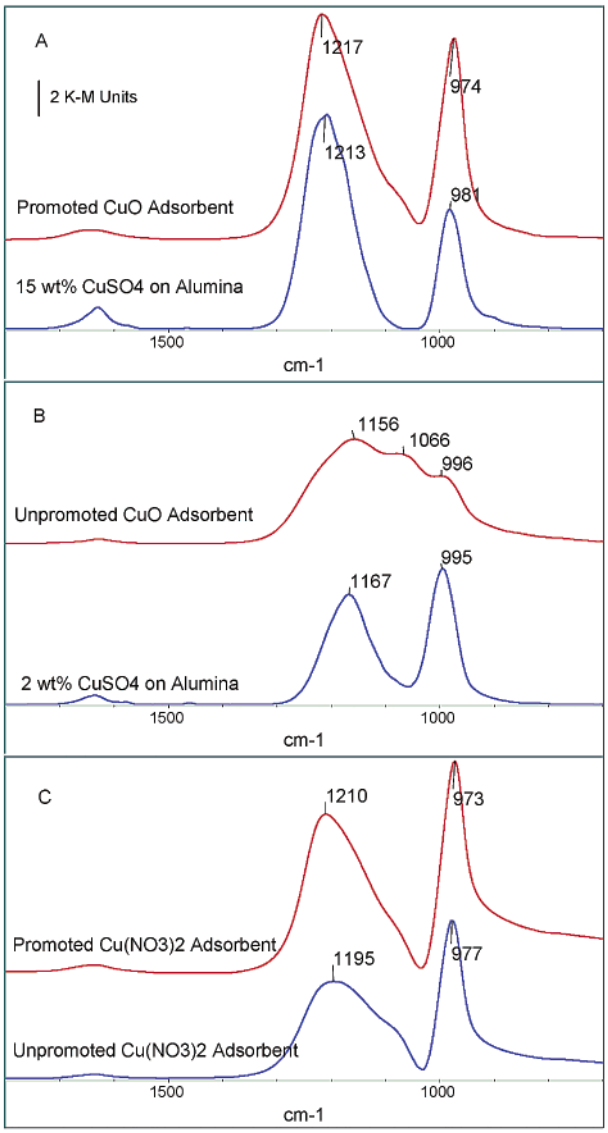

Figure 5. Diffuse reflectance infrared spectra of the unpromoted and HCl-promoted CuO adsorbents and unpromoted and HCl-promoted $Cu(NO_3)_2$ adsorbents after sulfation. The spectra of the sulfated adsorbents are all referenced to the same vertical scale in Kubelka–Munk units (see vertical bar in spectrum A). The spectra of alumina treated with $CuSO_4$ are shown with an adjusted vertical scale to aid comparison.

about 60%, with a lower overall capacity. On MgO and TiO_2, two other support materials tested, the enhancement was less than 25% with added chloride.

Diffuse Reflectance Infrared Spectra of Sulfated Adsorbents. The diffuse reflectance infrared spectra of four different adsorbents, the unpromoted and HCl-promoted CuO and $Cu(NO_3)_2$ adsorbents, after exposure to the SO_2/O_2 reaction gas mixture are shown in Figure 5. Included in Figure 5 are spectra of alumina impregnated with $CuSO_4$. The spectra of the sulfated adsorbents are all shown with the same vertical scale (in Kubleka-Munk units), whereas the spectra of the $CuSO_4$ impregnated alumina have been adjusted to make comparisons easier. The sample that contains 15 wt % of $CuSO_4$ on alumina has a surface concentration of approximately 2.5 molecules/nm^2, whereas the 2 wt % $CuSO_4$ sample has a surface concentration of approximately 0.32 molecules/nm^2. Given that the surface site density on alumina is approximately 4 sites/nm^2, the 15 wt % $CuSO_4$ sample could very nearly saturate the surface sites.

The spectra in Figure 5 are grouped in a way to facilitate their comparison. The two main bands are due to the ν_3 absorption (1150−1220 cm^{-1}) and the ν_1 absorption (970−1000 cm^{-1}) of the SO_4^{2-} group.[5,12] However, there is significant potential for error in the bands below 1000 cm^{-1} due to the strong alumina absorption that occurs in this region. Thus, the intensities of bands below 1000 cm^{-1} must be treated very cautiously. As can be seen in Figure 5A, the sample of the HCl-promoted CuO adsorbent after sulfation shows bands that are very similar to those of the sample containing 15 wt % $CuSO_4$ on alumina, and the spectrum shows very little contribution from other species. On the other hand, after sulfation, the unpromoted CuO on alumina adsorbent shows bands for ν_1 and ν_3 that are similar in frequency to the 2 wt % $CuSO_4$ on alumina sample, Figure 5B, as well as a significant absorption at 1066 cm^{-1}.

The spectrum of the unpromoted CuO/Al_2O_3 adsorbent appears to be a mixture of at least two different components, including copper sulfate and sulfite species responsible for the absorptions at 1156 and 1066 cm^{-1}. The absorption observed at 1066 cm^{-1} is similar to a band observed when SO_2 is allowed to adsorb on aluminum oxide in the absence of oxygen and is assigned to chemisorbed SO_2 on aluminum oxide (a sulfite-like form).[9,10,13,14] With regard to the 1156 cm^{-1} absorption, Waqif et al. found a strong absorption at 1165 cm^{-1} after sulfating bulk copper oxide (using SO_2 and O_2) and after impregnating alumina with large amounts of $Cu(SO_4)$.[1]

The spectra of the promoted and unpromoted $Cu(NO_3)_2$ adsorbents after exposure to the SO_2/O_2 gas mixture, Figure 5C, show features that appear to be intermediate between the spectra of the two CuO adsorbents, with the promoted $Cu(NO_3)_2$ adsorbent appearing most like the promoted CuO adsorbent, and the spectrum of the unpromoted $Cu(NO_3)_2$ adsorbent looking most like that of the unpromoted CuO adsorbent. In addition, none of the spectra contain features that would indicate the formation of significant amounts of aluminum sulfate.[1,5,9] The infrared intensities indicate that the HCl-promoted CuO adsorbent shows the greatest formation of copper sulfate, and it is sequestered as copper sulfate with no apparent contribution from aluminum sulfate.

Infrared Results from Probe Molecule Adsorption. CO is a valuable probe of the metal oxidation state for a number of supported transition metal catalysts and, particularly, for supported copper materials. An extensive database exists for the frequencies that are observed for CO adsorbed on Cu^0, Cu^{1+}, and Cu^{2+} sites, although by far the oxidation state that adsorbs CO most effectively is Cu^{1+}.[15−19] As a general guide, CO adsorbed on Cu^0 sites shows an absorption maximum at frequencies of 2110 cm^{-1} and lower, CO adsorbed on Cu^{1+} sites shows an absorption maximum between 2110 and 2140 cm^{-1}, and CO adsorbed on Cu^{2+} sites typically shows an absorption maximum at frequencies above 2140 cm^{-1}. A similar, although not as extensive, database exists for NO adsorbed onto supported copper catalysts.[17−21] Unlike CO, NO adsorbs most effectively onto Cu^{2+} sites.

In Figure 6 are presented the spectra of CO adsorbed on promoted and unpromoted CuO and $Cu(NO_3)_2$ adsorbents. As can be seen, the promoted CuO adsorbent shows by far the largest uptake of CO, even when compared to the promoted $Cu(NO_3)_2$ adsorbent, showing that this material has the largest amount of available Cu^{1+}. It can also be seen that the promoted materials have significantly more Cu^{1+} available and less Cu^0 than the unpromoted materials.

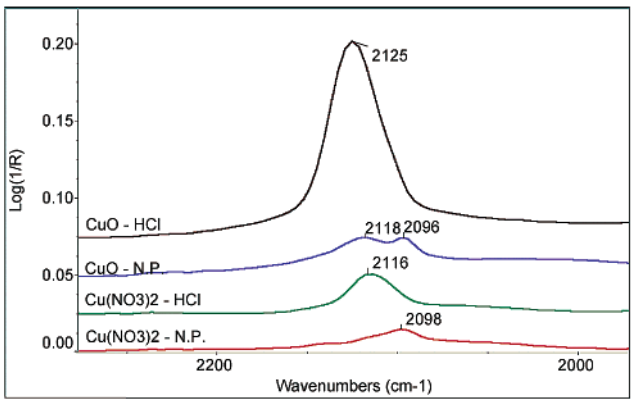

Figure 6. Infrared spectra of CO adsorbed on the unpromoted and HCl-promoted CuO and $Cu(NO_3)_2$ adsorbents. The spectra are referenced to the same vertical scale and are offset to aid viewing. The baseline of each spectrum coincides with its zero on the vertical scale.

The spectra of NO interacting with promoted and unpromoted copper oxide on alumina (not shown) yield the same general conclusion. The spectra obtained for HCl-promoted materials are consistent with the presence of Cu^{2+} sites on the surfaces of the promoted materials, with a well-defined absorption band at 1877 cm^{-1}, indicating the formation of a $NO-Cu^{2+}$ complex. The promoted CuO adsorbent shows a much larger band for the $NO-Cu^{2+}$ complex, with an integrated area 2.5 times greater than that of the promoted $Cu(NO_3)_2$ adsorbent, indicating that a much larger amount of the Cu^{2+} is available for interaction with NO on the promoted CuO adsorbent. An infrared band due to NO interacting with copper aluminate has been proposed in the literature, but no evidence for that interaction was observed in the current study.[18,20] Also, no absorption band for a $NO-Cu^{2+}$ complex is observed in the spectra for either of the unpromoted materials.

The infrared results from the CO and NO chemisorption experiments clearly show that there are more available Cu^{1+} and Cu^{2+} sites on the alumina surface of the promoted material, with the promoted CuO adsorbent containing the highest number of available adsorption sites.

Discussion

The TGA results provide clear evidence that chloride acts as a promoter for SO_2 uptake by supported CuO adsorbents. Centi et al. used very similar experiments to examine the kinetics of the SO_2 adsorption and reaction process on alumina-supported copper oxide adsorbents at 250−350 °C.[6] In that work, several different models for the adsorption and reaction of SO_2/O_2 mixtures on alumina-supported copper oxide were examined. The preliminary models involved adsorption and oxidation at copper sites and at aluminum sites, either in parallel or consecutively, forming copper sulfate and aluminum sulfate at the copper oxide/alumina interface. The models were either first or second order in the surface sites. Parallel reaction models that were second order in the concentration of copper sites and first or second order in aluminum sites proved to be successful at reproducing the observed results for S:Cu < 1, whereas the model that yielded the best fit for all S:Cu ratios involved an initial preequilibrium of SO_3 adsorbed at copper sites, followed by reaction to form copper sulfate or migration to nearby aluminum sites to form sulfate species at the copper oxide/alumina interface, eqs 1−3. Using the activation energies developed by Centi et al., virtually no interfacial sulfate is predicted to be formed at the temperature used in the current study, consistent with the infrared data of Figure 5. Thus, the model that was chosen to fit to the data is second order in copper sites, with no formation of interfacial sulfate, and the observed weight gain is assumed to follow the formation of $CuSO_4$.

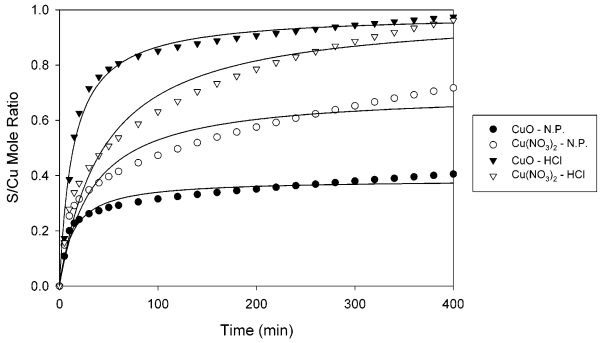

Figure 7. Adsorption/reaction of SO_2 on four different adsorbents. The circles are for the unpromoted adsorbents (N.P.), and the inverted triangles are for the promoted adsorbents. The solid symbols are for the adsorbents formed using CuO as the copper source, whereas the open symbols are for adsorbents prepared using $Cu(NO_3)_2$. The data points represent the experimental values, whereas the curves are the best fits of the kinetic model, eq 6.

TABLE 3: Parameters for Fit of Adsorption Data to Model[a]

formulation	R	κ	k
CuO − N. P.	0.385 ± 0.006	13.3 ± 1.4	74.7
CuO − HCl	0.985 ± 0.009	13.8 ± 0.8	72.0
$Cu(NO_3)_2$ − N. P.	0.702 ± 0.02	32.9 ± 4.5	30.2
$Cu(NO_3)_2$ − HCl	0.998 ± 0.03	44.7 ± 4.7	22.2

[a] Estimates of the standard deviation associated with the fit to the model are included.

In Figure 7, the thermogravimetric data collected for the third adsorption cycle (after three reduction treatments and two adsorption treatments) are shown for the four different adsorbents: the promoted and unpromoted CuO and $Cu(NO_3)_2$ adsorbents. The curves represent a fit of the data to the following function, which represents the model discussed above:

$$\frac{[SO_4^{-2}{}_{(surf)}]}{[CuO_{(surf)}]} = R\frac{t}{\kappa + t} \tag{6}$$

$$\text{where } \kappa = \frac{1}{k[CuO_{(surf)}]_0} \tag{7}$$

R and κ are allowed to vary to achieve the best fit to the data, as determined by minimizing the sum of the squares of the deviations between the predicted and observed values. κ is inversely proportional to the rate constant, defined in eq 7, and k is the net rate constant associated with the formation of $CuSO_4$, eqs 1 and 2. R is a parameter that reflects the availability of the copper sites on the surface for participation in the formation of copper sulfate ($R = 1$ if all of the copper on the surface can form $CuSO_4$). The calculated values of R and κ are shown in Table 3.

As can be seen from Figure 7, the model fits the data for the CuO adsorbents relatively well. However, the $Cu(NO_3)_2$ data exhibit a long-term weight gain that is apparently not accounted for in the present model. R is equal to 1, within experimental error, for the two chloride-promoted materials and significantly less than 1 for the two unpromoted materials, with the lowest value for R found, as expected, for the unpromoted CuO adsorbent. These are exactly the results expected if chloride acts by enhancing the dispersion of CuO on the support.

The rate constants for $CuSO_4$ formation can be calculated from κ. The kinetic treatment assumes that the concentration

of SO_2 is constant throughout the sample, and experiments using different volumes of sample were conducted to verify that these conditions were met as well as to verify that mass transport was not limiting. In the current work, the adsorbents are 8.0 wt % copper oxide (1.01×10^{-3} mol/g), $[SO_2] = 0.3\%$ (vol), and $[O_2] = 2\%$ (vol). Based on the results of Centi et al., the rate should not be dependent on $[O_2]$ in the concentration range used in these experiments but should show some dependence on $[SO_2]$, so that the rate constant, k, in eq 7 is actually $k = k'[SO_2]^a$, where the exponent, a, is between 0 and 1. Using $[Cu_{(surf)}]_0 = 1.01 \times 10^{-3}$ mol/g, k is determined to be 74.7 for the nonpromoted CuO adsorbent and 72.0 for the HCl-promoted CuO adsorbent. These rate constants are in good agreement, indicating that the chloride does not seem to affect the rate constant. The rate constants determined for the $Cu(NO_3)_2$ adsorbents are significantly lower than those for the CuO adsorbents. However, the secondary, long-term weight gain observed for the $Cu(NO_3)_2$ adsorbents distorts the calculation of the rate constants, and these rate constant determinations cannot be viewed with as much confidence as those for the CuO adsorbents.

Chloride Promotion. The interpretation that the promoting effect of chloride is to increase the copper oxide dispersion is supported by the following results from this study:

(1) The rapid uptake and 1:1 limiting S:Cu stoichiometry for the adsorption process for the promoted adsorbents;

(2) The near unity values determined for R, the copper availability parameter, from the kinetic analysis (related to 1 above);

(3) The lack of any significant amount of bulk copper sulfate observed in the infrared spectra of the promoted adsorbents; and

(4) The much higher availability of surface copper sites for the promoted adsorbents measured by the infrared studies of CO and NO probe molecule adsorption.

For the CuO adsorbents, the dominant effect of chloride promotion can be explained by an increase in the dispersion of the copper oxide species, although even the promoted $Cu(NO_3)_2$ adsorbent shows a higher rate of adsorption and higher capacity for SO_2, more available copper, than does the unpromoted $Cu(NO_3)_2$ adsorbent. The unpromoted CuO adsorbent shows a lower limiting S:Cu stoichiometry presumably because many of the Cu species are unavailable initially, lying under the topmost CuO layer. Some of the underlying copper may participate, however, and the migration of sulfate from the surface to the bulk is proposed to account for the infrared absorptions similar to those assigned to bulk $CuSO_4$ by Waqif et al.[1] The infrared spectrum of the unpromoted $Cu(NO_3)_2$ adsorbent shows characteristics similar to that of the unpromoted CuO adsorbent, indicating the likely formation of bulk copper sulfate in the case of this adsorbent, and supporting the idea that chloride has an effect on dispersion even for adsorbents prepared using $Cu(NO_3)_2$. This interpretation is completely consistent with the values of R calculated from the kinetic model for the different adsorbents. However, the effect of chloride is not solely accounted for by dispersion because the rate of uptake for the chloride-promoted CuO adsorbent is initially much more rapid than that of either of the $Cu(NO_3)_2$ adsorbents. It is important to note that the differences between the promoted adsorbents prepared using CuO and those prepared using $Cu(NO_3)_2$ persist after many adsorption/regeneration cycles, indicating that the unique adsorption characteristics of the promoted adsorbents are stable.

It is proposed that the mechanism whereby the chloride increases the dispersion of the adsorbents is that the chloride enhances wetting of the alumina surface by copper sulfate and/or copper oxide. It is suggested that copper oxide or copper sulfate domains on the alumina surface spread out over the surface during the initial calcining and/or adsorbent regeneration steps. This is consistent with the results observed for the promoted CuO adsorbents (see Figure 4) that show that two to three adsorption/regeneration cycles are required before the adsorbents develop their maximum adsorption capacity. This model also explains the enhancement observed for the promoted $Cu(NO_3)_3$ adsorbent. At the relatively high weight loadings examined, it is expected that there will be some CuO crystallite formation even when using the $Cu(NO_3)_3$ precursor. The addition of chloride to these adsorbents could allow the copper oxide/sulfate domains to spread out on these adsorbents as well, yielding the enhanced adsorption characteristics for these adsorbents compared to the unpromoted $Cu(NO_3)_3$ adsorbents.

It is suggested that the difference between the promoted adsorbents prepared using CuO and those prepared using $Cu(NO_3)_3$ is also explained by this model and is due to the much larger extent of the CuO domains formed on the promoted CuO adsorbents. The adsorbents formed using $Cu(NO_3)_3$ presumably have a significant fraction of the surface copper present as isolated species, perhaps as small copper aluminate ($CuAl_2O_4$) domains. For the adsorbents prepared from CuO, however, as the CuO spreads out over the surface, much if not all of the copper may still be contained in extended CuO networks on the surface. It is believed that these extended networks facilitate the adsorption and oxidation of SO_2, resulting in more rapid SO_2 adsorption and higher adsorption capacities. The extended CuO network may also explain the apparently much higher values for available Cu^{1+} and Cu^{2+} observed for the promoted CuO adsorbents in the probe molecule adsorption experiments, by facilitating the oxidation or reduction of copper adsorption sites, as needed, to yield a surface that is much more active for the adsorption of CO or NO.

Conclusions

Chloride has been observed to be a strong promoter for low-temperature (150 °C) adsorption of SO_2 from oxygen-containing gas streams. From our results, it is clear that chloride is the promoter, not an alkali metal, and that the enhancement observed in terms of capacity for SO_2 adsorption is more than 100% for adsorbents formed using CuO as the copper source. The adsorbents formed using CuO and promoted with chloride yield the most rapid uptake of SO_2 for short-term exposures including exposure times as long as 6 h. It is found that the primary way that chloride acts is by increasing the dispersion of the CuO species, with the resulting increased dispersion stable for many adsorption/regeneration cycles. It is suggested that the increased dispersion is realized by the chloride enhancing the wetting of the alumina surface by the copper oxide or copper sulfate species, resulting in the copper species spreading out over the surface, and forming extended CuO networks on the alumina surface.

References and Notes

(1) Waqif, M.; Saur, O.; Lavalley, J. C.; Perathoner, S.; Centi, G. *J. Phys. Chem.* **1991**, *95*, 4051.

(2) Jeong, S. M.; Kim, S. D. *Ind. Eng. Chem. Res.* **1997**, *36*, 5425.

(3) Yoo, K. S.; Kim, S. D.; Park, S. B. *Ind. Eng. Chem. Res.* **1994**, *33*, 1786.

(4) Yoo, K. S.; Jeong, S. M.; Kim, S. D.; Park, S. B. *Ind. Eng. Chem. Res.* **1996**, *35*, 1543.

(5) Centi, G.; Passarini, N.; Perathoner, S.; Riva, A. *Ind. Eng. Chem. Res.* **1992**, *31*, 1947.
(6) Centi, G.; Passarini, N.; Perathoner, S.; Riva, A. *Ind. Eng. Chem. Res.* **1992**, *31*, 1956.
(7) Moskovitz, M. L.; Kepner, B. E. U.S. Patent 6,338,830 to Apyron Technologies, Inc., 2002.
(8) Moskovitz, M. L.; Kepner, B. E. U.S. Patent 5,948,726 to Project Earth Industries, Inc., 1999.
(9) Mitchell, M. B.; Sheinker, V. N.; White, M. G. *J. Phys. Chem.* **1996**, *100*, 7550.
(10) Mohammed Saad, A. B.; Saur, O.; Wang, Y.; Tripp, C. P.; Morrow, B. A.; Lavalley, J. C. *J. Phys. Chem.* **1995**, *99*, 4620.
(11) Bolli, R. E.; Woods, M. C.; Madden, D. R.; Corfman, D. W. In *Processing and Utilization of High-Sulfur Coals V*; Parekh, B. K., Groppo, J. G., Eds.; Elsevier Science Publishers: Amsterdam, The Netherlands, 1993; p 437.
(12) Ferraro, J. R.; Walker, A. J. *J. Phys. Chem.* **1965**, *42*, 1278.
(13) Saur, O.; Bensitel, M.; Mohammed Saad, A. B.; Lavalley, J. C.; Tripp, C. P.; Morrow, B. A. *J. Catal.* **1986**, *99*, 104.
(14) Datta, A.; Cavell, R. G.; Tower, R. W.; George, Z. M. *J. Phys. Chem.* **1985**, *89*, 443.
(15) Dandekar, A.; Vannice, M. A. *J. Catal.* **1998**, *178*, 621−639.
(16) Dandekar, A.; Vannice, M. A. *Appl. Catal. B* **1999**, *22*, 179−200.
(17) Fu, Y.; Tian, Y.; Peiyan, L. *J. Catal.* **1991**, *132*, 85.
(18) Lokhov, Y. A.; Morozov, L. N.; Davydov, A. A.; Kostrov, V. V. *Kinet. Katal.* **1980**, *21*, 1295−1298.
(19) Lokhov, Y. A.; Davydov, A. A. *Kinet. Katal.* **1979**, *20*, 1498−1505.
(20) Hierl, R.; Urbach, H.-P.; Knözinger, H. *J. Chem. Soc., Faraday Trans.* **1992**, *88*, 355−360.
(21) Pozdnyakov, D. V.; Filimonov, V. N. *Kinet. Katal.* **1973**, *14*, 760−766.